ISSN 0023-1584, Kinetics and Catalysis, 2012, Vol. 53, No. 5, pp. 632–639. © Pleiades Publishing, Ltd., 2012.
Original Russian Text © V.V. Danilevich, L.A. Isupova, A.P. Kagyrmanova, I.V. Kharina, D.A. Zyuzin, A.S. Noskov, 2012, published in Kinetika i Kataliz, 2012, Vol. 53, No. 5, pp. 673–680.

RUSSIAN CONGRESS ON CATALYSIS "ROSKATALIZ"

Highly Effective Water Adsorbents Based on Aluminum Oxide

V. V. Danilevich, L. A. Isupova, A. P. Kagyrmanova, I. V. Kharina, D. A. Zyuzin, and A. S. Noskov
Boreskov Institute of Catalysis, Siberian Branch, Russian Academy of Sciences, Novosibirsk, 630090 Russia
e-mail: dvv@catalysis.ru

Received November, 28, 2011

Abstract—A method of preparation of a stable, high performance water adsorbent with the phase composition η-Al_2O_3 + γ-Al_2O_3 + χ-Al_2O_3 from thermally activated hydrargillite has been developed. The synthesis procedure does not involve a reprecipitation stage. The resulting adsorbent has a high specific surface area (400 m^2/g) and a mean pore diameter of 3.5 nm or below. The static capacity of the adsorbent reaches 24.2 g H_2O per 100 g of sorbent, and its dynamic capacity is 8.2 g H_2O per 100 g of sorbent. Service life tests showed the stability of the adsorbent in multiple sorption–desorption cycles. The minimum dew point in drying is –58.8°C.

DOI: 10.1134/S0023158412050059

Sorption processes are used in the modern gas, petrochemical, and chemical industries to improve the product quality and to carry out fine purification and drying of process streams. Sorption is used in the transportation of natural gas, in the production of oxygen, and in some other technologies such as reforming and hydrocracking [1, 2].

Dehumidification of streams of gas or liquid is important to prevent condensation and freezing of water in industrial pipelines and equipment; to rule out corrosion of process equipment; to prevent undesirable chemical reactions such as hydration, and hydrolysis; to prevent the poisoning of the catalyst and maintain it in operable condition [2, 3].

In order to perform the selective adsorption of water from a gas or liquid stream, solid-phase adsorbents are used: zeolites, silica gels, and activated alumina. These sorbents are produced in Russia and abroad and are available in abundance in the domestic market. Typically, the adsorption processes that are used in the dehumidification of gas streams are based on cyclic variation of temperature (thermal swing adsorption, TSA) or pressure (pressure swing adsorption, PSA). These processes include the regeneration of the adsorbent, which consists of sorption and desorption stages, allowing the adsorbent to be multiply reused in dehumidification.

With the steadily growing demand for zeolite and silica gel dehumidifiers in the petrochemical and gas industries, the adsorbents based on activated alumina has been relegated to the background in spite of their thermal stability, high mechanical strength, and resistance to condensed moisture and the availability of raw materials for their production [4]. In addition, even at a high relative humidity, alumina adsorbents show high adsorption capacity that 1.5–2 times exceeds the capacity of zeolites under the same conditions [3].

One of the possible reasons for the decline of interest in alumina sorbents is the fact that the domestic industry still produces insufficiently efficient γ-Al_2O_3-based sorbents that have a low specific surface area (about 250 m^2/g). Besides, γ-Al_2O_3 is produced via an outdated technology based on hydrargillite reprecipitation for pseudoboehmite formation, which is accompanied by the formation of a large amount of chemically contaminated wastewater. The insufficiently large surface area and the absence of micropores makes these adsorbents inappropriate for drying of gas streams to a dew point of –40°C or below [5].

The sorption properties of water adsorbents can be improved by using tools and materials that are capable of forming a system of micropores and increasing the specific surface area of the alumina adsorbent. For this purpose, ultrafine, fine-pore, thermally activated aluminum hydroxide (TAH) can be used as the precursor. This material is obtained either by pulse heating of hydrargillite to the dehydration temperature under pneumatic transport conditions [6] or by using a centrifugal flash reactor (CEFLAR^{TM}) developed at the Institute of Catalysis, Siberian Branch, Russian Academy of Sciences [7, 8].

Previously, it was found that the hydration of the product of the centrifugal thermal activation of hydrargillite in an alkaline medium yields the bayerite phase in an amount of up to 80% (according to the X-ray diffraction data), depending on the duration of the operation [9]. This hydration product can be subjected to molding in an extrusion machine. Heat treatment of bayerite-containing aluminum hydroxide at 300–550°C yields the low-temperature aluminum oxide η-Al_2O_3 [4]. Heat treatment of bayerite at a lower temperature (as compared to heat treatment of pseudoboehmite, the precursor of γ-Al_2O_3) produces aluminum oxides with a developed surface and a large

Table 1. Characteristics of the thermal activation products of hydrargillite

Product of thermal activation	S_{BET}, m^2/g	V_{pore}, cm^3/g	LOI*, %	Phase composition,%			Average particle diameter, μm
				hydrargillite	boehmite	XAP** + χ-like Al_2O_3	
TAH	124	0.11	10.0	15	~1	84	57.8
CTA-9 (after grinding)	178	0.13	5.2	2	–	98	18.9
CTA-15 (after grinding)	186	0.14	7.9	4	7	89	19.1

* Loss on ignition at 1000°C.

** X-ray amorphous phase.

Table 2. Aluminum hydroxide synthesis conditions

Hydration product	Initial sample for thermal activation	Hydrating solution	pH	Hydration method	Hydration temperature, °C	Hydration time, h
SW-1	TAH	NH_4OH	10	ball mill	22–24	24
SW-2	CTA-15 (ground)	"	"	stirred reactor	70–95	4
SW-3	"	NaOH	12	"	"	"
SW-4	TAH (ground)	"	"	"	"	"
SW-5	CTA-9 (ground)	NH_4OH	10	ball mill	22–24	24

number of micropores. The technology for bayerite-containing aluminum hydroxide production from TAH is also characterized by a much smaller volume of waste and is, therefore, an environmentally more attractive option.

The aim of this work was to develop a technology for preparing highly efficient water adsorbents based on low-temperature phases of alumina, mainly η-Al_2O_3, obtained by thermal activation of hydrargillite and its subsequent hydration, extrusion molding, and thermal treatment.

EXPERIMENTAL

Water adsorbents were synthesized from the product obtained by thermal activation of hydrargillite in the experimental reactor CEFLAR™ or from commercially available, thermally activated aluminum hydroxide (OAO Achinsk Alumina Refinery, RF Specifications TU 1711-001-05785164-2002). In the former case, the synthesis of the CTA-9 product was performed in a centrifugal drum-type flash reactor at an electric heater temperature of 700°C, a drum rotation speed of 60 rpm, and a hydrargillite flow rate of 40 kg/h (hydrargillite was received from Achinsk Alumina Refinery). The CTA-15 product was obtained under the same conditions, but at a lower temperature of 650°C. The characteristics of the thermal activation products are listed in Table 1.

Preparation of Water Adsorbents

The hydration of CTA-9, CTA-15, and TAH was carried out in alkaline solutions using heated, vigorously stirred reactors or a laboratory ball mill with 1-L ceramic jars. Hydration in the ball mill was performed at a solid-to-liquid ratio of S : L = 1 : 1, a temperature of 22–24°C, and a hydration time of τ = 24 h in an NH_4OH solution. The thermal activation product was used in the unground state (~57 μm) or was crushed in a disintegrator (DESI-15, Desintegrator Tootmise OÜ, Estonia). In hydration in the reactor, the ratio S : L ranged from 1 : 3 to 1 : 4. The process was conducted at 70–95°C and τ = 4 h in a solution of NaOH or NH_4OH. The powder was preliminarily ground in in the DESI-15 disintegrator to a particle size of 15–30 μm. The aluminum hydroxide synthesis conditions are specified in Table 2.

After the completion of hydration and separation of the solid and liquid phases on a nutsch filter at a reduced pressure usiing a layer of filter cloth, the solid was dried in an oven and was then plasticized (peptized) with nitric acid at an acid modulus of 0.1 (mol acide/mol Al_2O_3) in a mixer. The duration of this stage was determined by the time required to obtain a a plastic material (30–60 min) suitable for molding. At the next stage, the plastic mass was forced through the die of a ram extruder with a hole diameter of 4 mm to obtain finished pellets.

The pellets were loaded into a 5-L tubular furnace, were dried at 120°C for 24 h, and were then heattreated at 350–550°C in a stream of dry air (dew point no higher than –40°C, flow rate of 1000–5000 h^{-1}, heating rate of 50 deg/h). The duration of this stage after the establishment of the preset conditions was 4 h. After heat treatment, the pellets had a diameter of 3.75 ± 0.15 mm and a length of 5 ± 0.8 mm.

X-ray diffraction (XRD) was performed on an HZG-4 diffractometer (Zeiss, Germany) at a wavelength of 1.54184 Å in the point-by-point scanning mode ($2\theta = 10°–75°$, scan step of 0.1°, counting time of 10 s per data point). Because of the complexity of the quantitative determination of individual phases in a multiphase system (due to the similarity of their parameters), the products will be characterized in the tables in terms of $(\gamma + \eta)$-Al_2O_3, χ-Al_2O_3, and χ-like Al_2O_3 + X-ray amorphous phase contents.

Thermal analysis (TA) was performed on a Q-1500DY1T system (MOM, Hungary) in the temperature range of 20–1000°C in air at a heating rate of 10 deg/min. The sample weight was 100 mg, and the accuracy of weight loss measurements was ±0.5%. The TA method of quantitative determination of the phase composition of hydrated products is described in the literature [5].

Textural characteristics of CTA products, TAH, and adsorbents were derived from nitrogen adsorption isotherms at 77 K. The specific surface area was measured by the BET method; the micropore volume, by the *t*-method. TThe volume of mesopores was determined by analyzing the integral curve of pore volume distribution over pore radius (in the adsorption branch). The mean pore diameter was calculated uisng the equation $d_{\text{mean}} = 4000V_{\text{pore}}/A$, where A is the specific surface area of the pellets [10]. The mechanical strength of the pellets was estimated by measuring the force that caused pellet breakup as a result of coaxial compression between two parallel planes perpendicular to the pellet axis. The tests were performed on 30 pellets of each sample.

For comparative experiments, we synthesized, via a well-known hydrargillite reprecipitation procedur aimed at obtaining pseudoboehmite [11], γ-Al_2O_3 as cylindrical pellets. After calcination, the pellets had a diameter of 3.8 ± 0.1 mm and a length of 4.9 ± 0.7 mm.

Determination of the Static Water Vapor Capacity of the Adsorbents

Static water capacity of the adsorbents was determined as the mass of water adsorbed by a unit mass of absorbent at adsorption equilibrium at 25°C in an atmosphere with a relative humidity of 60%. This humidity was produced in a closed space over a saturated aqueous solution of sodium bromide after evacuation for 30 min. The static adsorption capacity of a material was determined on two samples, about 2.5 g each, weighed in closed calibrated vials with an accuracy of 0.0001 g.

The static capacity was calculated using the formula

$$\mathrm{SC} = \frac{\Delta m}{m} \times 100,$$

where SC is the static capacity of the sorbent (g H_2O/100 g sample), Δm is the amount of adsorbed water (g) at adsorption equilibrium, and m is the weight of the sample. Equilibration was monitored every 24 h by withdrawing the sample from the desiccator and weighting it. After the complete saturation of the adsorbent with water vapor was reached, the experiment was stopped. The static capacity of the adsorbent was determined as the arithmetic mean of two replica measurements. The maximum allowable difference between the measurements was 0.1% at a confidence probability of $P = 0.95$.

Determination of the Dynamic Water Vapor Capacity of the Adsorbents

The dynamic capacity of the adsorbents was determined by as the mass of water absorbed by a unit mass of adsorbent at the instant the gas leaving the adsorber reached a dew point of –40°C. The measurements were made under the following conditions: moisture content of the gas fed into the adsorber, 15.6–16.6 g/m^3 (dew point of 18.5–19.5°C); volumetric flow rate of the air–vapor mixture, 8.7 L/min; atmospheric pressure; 23°C; adsorbent volume, 200 cm^3 (133–145 g); inner diameter of the adsorber, 30 mm, adsorber height, 400 mm.

The dew point was determined on a Cermet II hygrometer (Michell Instruments, United Kingdom), whose measurement range is –100 to +20°C).

Dynamic water vapor adsorption capacity was calculated as

$$\mathrm{DC} = \frac{\Delta m}{m} \times 100,$$

where DC is the dynamic capacity of the sorbent (g H_2O/100 g sample), Δm is the amount of adsorbed water (g) during the test, and m is the weight of the test sample (g).

Service Life Tests

The service life tests were carried out to determine the effect of hydrothermal aging on the sorption and textural characteristics of the water adsorbents after five adsorption–desorption cycles.

An air stream saturated with water vapor in a bubbler was fed into the adsorber, which contained 1.4 L (1.02 kg) of the adsorbent (Fig. 1). The air was supplied at a rate of 200 L/h in the first cycle and at a rate of 400 L/h in the subsequent cycles. The volume of the adsorber was 1.5 L (inner diameter of 52 mm, height of 0.7 m). The relative humidity of the air stream to be dried was ~40% in the first cycle and no less than 90%

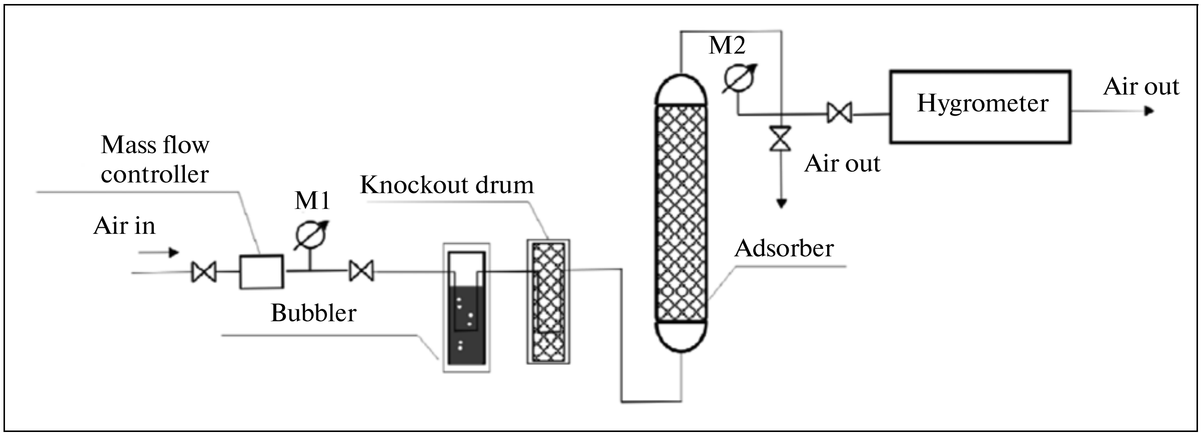

Fig. 1. Experimental setup for service life tests of water adsorbents.

in the subsequent cycles at atmospheric pressure and a temperature of 23°C.

As the humid air was passing through the adsorbent bed, it dried. The air stream leaving the adsorber was directed to the hygrometer to measure the humidity of the dry air.

The tests were continued until the humidity of the gas at the outlet of the adsorber had a dew point of –40°C. Thereafter, the dynamic capacity of the sorbent was determined gravimetrically. After the completion of the sorption cycle, the sorbent was regenerated in a tubular furnace in flowing dry air for 8 h at 250°C.

RESULTS AND DISCUSSION

According to XRD data, the hydration of TAH in an NH_4OH medium under wet grinding conditions in a ball mill for 24 h at room temperature ("cold hydration"), reduces the amorphous phase + χ-like Al_2O_3 content of the material to 35% and yields 51 wt % bayerite (sample SW-1, Table 3). In the hydration of ground CTA-9 (sample SW-5) under the same conditions, no bayerite formation was observed, but 19 wt % pseudoboehmite formed. It was shown earlier [12] that a decreasing particle size has an adverse effect on the hydration of TAH under bayerite formation conditions at temperatures around 100°C. Apparently bayerite practically does not form in the fine fraction of the CTA product (TAH analogue) under mild conditions at room temperature. In the product of hydration of CTA-15 (pre-ground in the disintegrator down to 15–35 μm) in NH_4OH at 70–95°C ("hot hydration") for 4 h, the amorphous phase and the χ-like Al_2O_3 phase were not detected. The amount of the resulting bayerite was somewhat smaller than in the case of SW-1, while the pseudoboehmite was observed in an amount of 34% (SW-2 sample, Table 3). A product of similar phase composition resulted from the hot hydration of CTA-15 in a NaOH medium (SW-3 sample). However, this process yielded 13% more bayerite and 9% less pseudoboehmite. Apparently, the increase in the bayerite yield was due to the higher pH of the medium in hydration in NaOH.

The loss on ignition (LOI) values for samples SW-1, SW-2, SW-3 and SW-4 at 1000°C are almost equal and are 23.2, 23.0, 23.9, and 23.7% respectively. The LOI for sample SW-5 is significantly smaller (12%), which may be due to the low trihydroxide content of the hydration product. The increase in LOI to 23–24% (by a factor larger than 2) indicates a high degree of hydration of the products of the thermal activation of

Table 3. Phase composition of the hydrated products of the thermal activation of hydrargillite (according to XRD data)

Sample	LOI, %	Hydrargillite, %	Bayerite, %	Boehmite		Pseudoboehmite		χ-like Al_2O_3 + XAP		
				%	D*, Å	%	D*, Å	%	D*, Å	a**, Å
SW-1	23.2	13	51	1	150	–	–	35	55	7.900
SW-2	23.0	9	45	12	170	34	35	–	–	–
SW-3	23.9	7	58	10	120	25	35	–	–	–
SW-5	12.0	5	1	–	–	19	35	75	50	7.885

* Crystallite size.
** Unit cell parameter.

Table 4. Phase composition of the water adsorbents (according to XRD data)

Sample	Heat treatment, °C	γ- and η-Al_2O_3, %	χ-Al_2O_3		
			%	D, Å	a, Å
SW-1	450	35	65	45	7.890
SW-2	400	49	51	35	7.892
SW-3	″	57	43	45	7.914
SW-5	″	15	85	40	7.909
SW-5	500	25	75	″	7.906

Table 5. Textural and sorption characteristics of the water adsorbents as cylindrical pellets

Sample	Heat treatment, °C	S_{BET}, m^2/g	V_{micro}[a], cm^3/g	V_{meso}[b], cm^3/g	Pore diameter, nm	SC	DC	Mechanical strength[c], MPa
						g H_2O/100 g adsorbent		
SW-1	350	327	0.11	0.10	2.2	18.9	4.9	7.1
″	400	390	0.16	0.12	2.8	21.6	7.2	6.0
″	450	343	0.13	0.12	3.0	20.9	3.0	6.4
″	500	340	0.11	0.13	3.2	19.5	2.7	6.7
″	550	328	0.10	0.15	3.4	19.0	2.5	7.5
SW-2	400	407	0.23	0.21	3.5	24.2	7.5	6.3
SW-3	″	403	0.21	0.19	3.3	22.1	8.2	5.6
SW-4	″	356	0.19	″	3.5	21.7	6.3	6.2
SW-4-SL[d]	″	341	″	0.18	″	21.5	–	4.1
SW-5	″	330	0.15	0.26	4.5	19.7	2.7	9.5
″	500	282	0.12	0.29	5.2	18.1	–	9.1
g-Al_2O_3	–	294	0	0.67	9.2	11.8	1.8	4.7

[a] Micropore diameter below 2 nm (according to the IUPAC classification).
[b] Mesopore diameter of 2–50 nm.
[c] Crush strength.
[d] Sample SW-4 calcined at 400°C and subjected to service life tests.

hydrargillite (for comparison, the LOI for hydrargillite is 34.6%).

Due to the presence, in the SW-1–SW-5 samples, of pseudoboehmite and/or X-ray-amorphous hydroxide (hydrated χ-like Al_2O_3, which is apparently similar in composition to pseudoboehmite) and due to the formation of hydroxonitrate bonding on the surface of the fine aluminum hydroxides particles under the action of the plasticizer (nitric acid), the resulting plastic masses are moldable by extrusion into pellets with a diameter of 4 mm.

An X-ray diffraction analysis of the water adsorbents obtained by the thermal treatment of the hydroxides SW-1–SW-5 in a stream of dry air at 400–450°C, showed (Table 4) that the samples are not single-phase and consist mainly of the γ- and η-Al_2O_3 phases (15 to 57%) and χ-Al_2O_3 (43 to 85%). The boehmite phase was not observed in the calcined samples. The proportion of the γ- and η-Al_2O_3 is higher in those samples whose hydroxide precursors contained more bayerite and pseudoboehmite.

Table 5 shows the textural characteristics of the water adsorbents prepared under different hydration and heat treatment conditions. As the calcification temperature of the samples obtained from the hydroxide SW-1 is increased, the specific surface area passes through a maximum at 400°C (Fig. 2), which is explained by the almost complete decomposition of the hydroxides in the sample calcined at this temperature and by the formation of fine-particle low-temperature aluminum oxide phases (η-, γ-, and χ-Al_2O_3). At higher calcination temperatures, the specific surface area decreases due to sintering. As a result, the mean pore size and the mesopore volume increase and the micropore volume decreases.

Raising the hydration temperature for the products of thermal activation hydrargillite from 22–24 to 70–95°C leads to the formation of aluminum oxides with a larger micropore volume (Table 5, SW-2–SW-4,

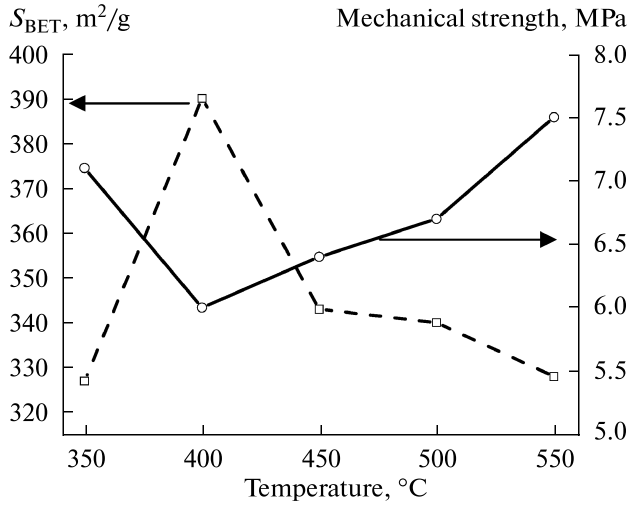

Fig. 2. Dependence of the specific surface area and mechanical strength of the SW-1 adsorbent on the heat treatment temperature.

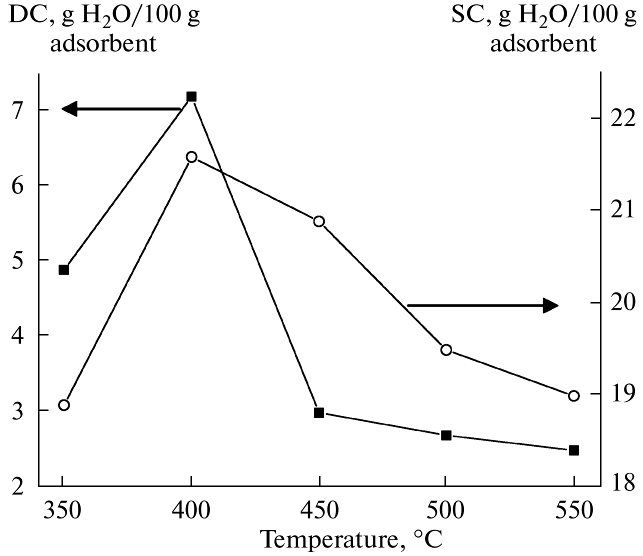

Fig. 3. Dependence of the static and dynamic water vapor adsorption capacities of the adsorbent on the temperature of heat treatment of SW-1 aluminum hydroxide pellets.

samples calcined at 400°C) than in the samples SW-1 and SW-5 hydrated at room temperature and calcined at 400°C. No significant affect of the nature of the electrolyte (NH_4OH or NaOH, samples SW-2 and SW-3 calcined at 400°C) on the textural characteristics of the product was observed.

With an increasing calcination temperature, the mechanical strength of the granular samples prepared from SW-1 varies non-linearly and has the minimum value (6.0 MPa) at a calcination temperature of 400°C. The changes in the mechanic strength (Fig. 2) are mainly due to the fact that the strength of a unit contact increases with increasing calcination temperature. This strength is sufficient for successful transportation, loading, and multicycle operation of the adsorbent in industrial adsorbers. The mechanical strength of all products of hot hydration after calcination at 400°C (SW-2–SW-4), as well as that of the sample SW-1, is ~6 MPa. This may indicate a higher strength of a unit contact in these samples at a larger mesopore volume, which is due to the high pseudoboehmite content of the hydroxide precursor.

The static water vapor capacity of all SW-1 samples at a relative humidity of 60% correlates with the specific surface area of the sorbent (Fig. 3). The highest static capacity, 21.6 g H_2O/100 g adsorbent, was observed for SW-1 calcined at 400°C. The static capacity of the hot-hydration samples (SW-2–SW-4) varies from 21.7 to 24.2 g H_2O/100 g of adsorbent and also correlates with their specific surface area (Table 5).

The dynamic water vapor capacity of the samples that were calcined at 400°C varies in a wide range (2.7–8.2 g H_2O/100 g adsorbent, Table 5) and apparently depends not only on the specific surface area. It can also depend on the micropore volume, mean pore diameter, phase composition, and/or acid–base properties of the adsorbents. For example, we observed a significant decrease in the dynamic capacity of the samples with a mean pore diameter of 4.5 nm (sample SW-5 calcined at 400°C, Table 5), and this can be explained by a decrease in the contribution from capillary condensation to the overall adsorption. According to the Kelvin equation [1], capillary condensation in the pores of this size only occurs at a relative humidity higher than 65%. Given that dynamic adsorption occurs in the sorption front, we can conclude that this humidity can be attained only in the initial (equilibrium) part of the front, while in the rest of the bed, relative humidity is significantly lower. It is also possible that the low dynamic capacity of this sample is due to its high χ-Al_2O_3 content (85%, see Table 4), since the original hydroxide SW-5 (Table 3) has no bayerite phase. Note that the high χ-Al_2O_3 content of the adsorbent (60%, SW-1 sample in Table 4) leads to a decrease in dynamic capacity even at a mean pore diameter of 3 nm (sample SW-1 calcined at 450°C, Table 5). In addition, we observed a correlation between the equilibrium capacity measured at low relative humidity (1–3%) and Brønsted acidity [13], which is higher in η-Al_2O_3.

The water sorbents examined here, even those calcined at 550°C, are superior in terms of static and dynamic capacity to the reference material γ-Al_2O_3, which contains no micropores and has a 2–3 times larger mean pore diameter (9.2 nm, Table 5). This demonstrates the great importance of the developed system of micro- and small mesopores in adsorbent for adsorption dehumidification.

Thus, water adsorbents based on the low-temperature forms of aluminum oxide (η-, γ-, and χ-Al_2O_3) were prepared from hydrargillite thermal activation

Table 6. Results of service life tests of adsorbent SW-4 calcined at 400°C

Cycle number	Relative humidity at the inlet, %	Residence time, s	Protective action time, h	DC, g H_2O/100 g adsorbent	Minimum dew point, °C
1	40	25.2	112	18.5	–58.8
2	90	12.6	26	16.8	–54.8
3	″	″	28	17.5	–53.4
4	″	″	″	17.8	–56.5
5	″	″	″	16.8	–56.7

products containing up to 60% bayerite that were hydrated in an alkaline medium. Due to the presence of micropores (with an overall mean pore diameter of <3.5 nm), these adsorbents are characterized by a high dynamic and static capacity and a higher mechanical strength as compared to the γ-Al_2O_3. The optimum temperature for calcination of bayerite-containing aluminum hydroxide is 400°C, since the finest alumina phase forms at this temperature.

The service life tests of the adsorbent SW-4 calcined at 400°C (analogue of SW-3) was performed using a special-purpose pilot plant (Fig. 1) designed at the Institute of Catalysis. The results of these tests are presented in Table 6. The maximum dynamic water vapor capacity was observed in the first cycle at an air–adsorbent bed contact time of 25.2 s and a relative air humidity of ~40% at the inlet of the adsorber. The minimum dew point of the gas dried in the adsorber was –58.8°C, and it was again achieved in the first cycle. As the contact time is shortened and the relative humidity of the gas flow is increased, the protective effect time of the adsorbent bed decreases sharply from 112 h in the first cycle to 26–28 h in the subsequent cycles. Simultaneously, the dynamic capacity of the adsorbent bed decreases by 9.2% (or, in absolute units, from 18.5 to 16.8 g H_2O/100 g adsorbent in the second and fifth cycles). Although the minimum dew point rises to –53.4°C in the third cycle, this temperature is quite sufficient for successful dehumidification of gas flows. However, the minimum dew point in cycles 2–5 is virtually unchanged and is within the measurement error of the Cermet 11 hygrometer. The ability of the adsorbent to adsorb water vapor under dynamic conditions also remains at a constant level during cycles 2–5 (within the error of measurement).

The textural characteristics and static water vapour capacity of sample SW-4-SL after the service life test (Table 5) differ little from those of the original sample, indicating that the adsorbent is stable over several adsorption–desorption cycles. However, its mechanical strength is reduced to 4.1 MPa, which could be attributed to the wedging effect of the water contained in micropores. However, under real operating conditions, the relative humidity of the gas entering the adsorber does not usually exceed a few percent and the micropores do not have time to be completely filled in deep dehydration; hence, the effect of wedging in the micropores on the strength of the sample can be neglected in this case.

Thus, we have developed highly effective water adsorbents based on low-temperature forms of aluminum oxide (η-, γ-, and χ-Al_2O_3). They are obtained by calcination of the alkaline hydration products of thermally activated aluminum hydroxide consisting largely of the bayerite phase (50% or more).

The water adsorbents obtained from bayerite-containing aluminum, as compared to those synthesized by classical γ-Al_2O_3 reprecipitation, have a more developed surface, contain micropores, and are mechanically stronger.

The textural characteristics of adsorbents depend on the hydration and heat treatment temperatures of the bayerite-containing aluminum hydroxide. The smallest pore diameter are observed for the water adsorbents obtained by the thermal activation and hydrated at room temperature. The largest values of specific surface area and micropore volume are obtained after calcination of aluminum hydroxide pellets in a stream of dried air at 400°C, at least 150°C below the calcination temperature of pseudoboehmite, the precursor of γ-Al_2O_3.

The sorption capacity of alumina adsorbents under the static and dynamic conditions depends primarily on their specific surface area. The dynamic capacity can also be affected by the phase composition and micropore volume of the drier.

The service life tests of the adsorbent SW-4 showed that the minimum dew point is virtually unchanged over a number of cycles and reaches a value of –58.8°C in the fifth cycle of the test. The textural characteristics and static water vapor capacity also do not undergo significant changes during the service life tests. This demonstrates the stability of the adsorbent and the possibility of efficient (almost complete) regeneration of the microporous adsorbents after each cycle.

REFERENCES

1. Kel'tsev, N.V., *Osnovy adsorbtsionnoi tekhniki* (Principles of Adsorption Engineering), Moscow: Khimiya, 1984.
2. Dąbrowski, A., *Adv. Colloid Interface Sci.*, 2001, vol. 93, nos. 1–3, p. 135.

3. Sircar, S., Rao, M.B., and Golden, T.C., *Stud. Surf. Sci. Catal.*, 1996, vol. 99, p. 629.
4. Stiles, A.B., *Catalyst Supports and Supported Catalysts: Theoretical and Applied Concepts*, London: Butterworths, 1987.
5. *Novyi spravochnik khimika i tekhnologa: Syr'e i produkty promyshlennosti organicheskikh i neorganicheskikh veshchestv* (Chemist's and Technologist's New Handbook: Raw Materials and Products of the Organic and Inorganic Compound Industries), Kalinkin, I.P., Ed., St. Petersburg: Mir i Sem'ya, 2002, part 1, p. 374.
6. Jovanovic, N., Novakovic, T., Janacovich, J., and Terlecki-Baricevic, A., *J. Colloid Interface Sci.*, 1992, vol. 150, no. 1, p. 36.
7. RF Patent 2264589, 2005.
8. RF Patent 2360196, 2009.
9. Kharina, I.V., Isupova, L.A., Litvak, G.S., Moroz, E.M., Kryukova, G.N., Rudina, N.A., Tanashev, Yu.Yu., and Parmon, V.N., *Kinet. Catal.*, 2007, vol. 48, no. 2, p. 327.
10. Gregg, S.J. and Sing, K.S.W., *Adsorption, Surface Area and Porosity*, New York: Academic, 1982.
11. Dzis'ko, V.A., Karnaukhov, A.P., and Tarasova, D.V., *Fiziko-khimicheskie osnovy sinteza okisnykh katalizatorov* (Physicochemical Foundations of the Synthesis of Oxide Catalysts), Novosibirsk: Nauka, 1978, p. 62.
12. Shkrabina, R.A., *Cand. Sci. (Chem.) Dissertation*, Novosibirsk: Inst. of Catalysis, 1982.
13. Zotov, R.A., Isupova, L.A., Glazyrin, A.A., Danilevich, V.V., Kharina, I.V., Zyuzin, D.A., and Volodin, A.M., *Kinet. Catal.*, 2012, vol. 53, no. 5, p. 570.